JOURNAL OF GUIDANCE, CONTROL, AND DYNAMICS
Vol. 38, No. 4, April 2015

General High-Altitude Orbit Corrections Using Electrostatic Tugging with Charge Control

Erik A. Hogan* and Hanspeter Schaub†
University of Colorado, Boulder, Colorado 80309

DOI: 10.2514/1.G000092

The use of an electrostatic force to perform general orbit corrections on a passive geosynchronous space object is investigated. Using inertial thrusters, a space tug approaches and settles into a piecewise fixed relative location with respect to a deputy object that needs to be towed to a new orbital location. Once in place, an electrostatic force is created between the two bodies using noncontact charge transfer, enabling the tugging craft to perform an inertial thrusting maneuver to modify the deputy orbit without physical contact. An open-loop analytical performance study is performed where variational equations are used to predict how much general orbital elements may be changed using this electrostatic force over one orbital period for a satellite at geosynchronous altitude. In contrast to earlier work, eccentric orbits and plane changes are also considered. The thrust direction issues associated with repositioning the tug craft during orbit modifications to achieve desired tugging force are also investigated. Numerical studies illustrate that even taking hours to maneuver the tug into a new pulling configuration only results in a few percent performance loss. Ranges of craft voltages are considered, as well as varying masses, illustrating promising deputy maneuverability.

Nomenclature

$a, e, i, \Omega, \omega, f$	=	orbital elements of deputy
a_c	=	component of deputy acceleration due to electrostatic force
F_c	=	electrostatic force between tug and deputy
k_c	=	coulomb constant (8.99×10^9 Nm^2/C^2)
L	=	separation distance between tug and deputy
m_d	=	mass of deputy object
n	=	mean motion of deputy
q_t, q_d	=	charges on tug and deputy, respectively
r_t, r_d	=	radii of tug and deputy, respectively
V_t, V_d	=	voltages on tug and deputy, respectively

I. Introduction

THE use of electrostatic forces for spacecraft formation maintenance, called coulomb formation flying, is a relatively new and intriguing area of research with a wealth of developments occurring in the last decade [1–5]. The use of electrostatic actuation in space is discussed as early as 1966 by Cover et al. [6]. The coulomb formation flying (CFF) concept revolves around active charge control of spacecraft to several kilovolts; at separation distances of tens of meters, these charge levels result in millinewtons of force. Through careful application of charging histories, the relative motion of spacecraft is affected for formation maintenance and reconfiguration [7–9]. A major benefit of CFF lies in its fuel and power efficiency. In the geosynchronous orbit regime, only watt levels of power are required to achieve the required charge levels, with specific impulses of 10^{10}–10^{13} s [2,6,10]. Furthermore, active charge control to the levels required for CFF has been demonstrated in flight. For example, on the spacecraft charging at high altitudes (SCATHA) mission, a spacecraft potential of 4 kV was achieved through emission of an electron beam at a current of 13 mA [11,12].

The vast majority of prior work with coulomb formation flying considers formations under the influence of electrostatic forces and gravity that evolve according to the resulting natural dynamics. However, it is not difficult to envision a scenario where a formation of spacecraft needs to perform an orbital maneuver, either for station keeping or due to a change in mission requirements. In a coulomb formation flying application, there are two ways to accomplish such a maneuver. One way would be for all spacecraft in the formation to possess individual thrusting capabilities, with each performing their maneuver separately. A more intriguing scenario is one where only a single craft in the formation possesses thrusting capability. A combination of electrostatic forces and thrusting (referred to as electrostatic tugging) could be used to tow the passive spacecraft and perform the necessary orbital maneuvers, as illustrated in Fig. 1. Here, an attractive electrostatic force is generated between the tugging vehicle and a deputy object. This virtual tether is then used to pull the deputy object while the tug performs a thrusting maneuver. Because of the small magnitude of electrostatic forces (millinewtons), low-thrust, long-duration tugging periods are required. This concept could also be applied to extend mission life for an otherwise functional spacecraft that has lost its ability to perform station keeping on its own.

The seminal work regarding the electrostatic tugging concept considers an application to geosynchronous Earth orbit (GEO) debris mitigation [5]. Here, variational equations are used to predict possible semimajor axis changes for debris objects under the influence of electrostatic tugging. No consideration is given to relative motion dynamics or charge control. Rather, an open-loop study is performed to assess the feasibility of raising a debris object on a circular geosynchronous orbit to a higher graveyard orbit. The results show that an object weighing several tons could be reorbited in a period of a few months. A follow-up study considers the relative motion and derives a control law to stabilize the relative positions of tug and debris during the towing period [13].

The requirements for active charge control are quite interesting when considering the electrostatic tugging concept, because noncooperative objects are not purpose designed for charge control. A method is needed to achieve the charges required for electrostatic tugging. This can be accomplished through the use of a directed electron beam, as illustrated in Fig. 1 [14]. In emitting a stream of negatively charged particles onto a remote object, the object becomes negatively charged due to the resulting electron current. At the same time, the tug is charged positive by the continuous emission of electrons. The opposite polarities of deputy and tug result in an attractive electrostatic force that, combined with low thrusting, allow for orbit modifications.

In the current study, a formation of two spacecraft is considered. One of the craft, denoted as the tug, possesses both thrusting and

Received 14 June 2013; revision received 21 November 2014; accepted for publication 25 November 2014; published online 17 February 2015.

*Graduate Student.

†Associate Professor, H. Joseph Smead Fellow, Aerospace Engineering Sciences; Chief Technologist, Wacari Group.

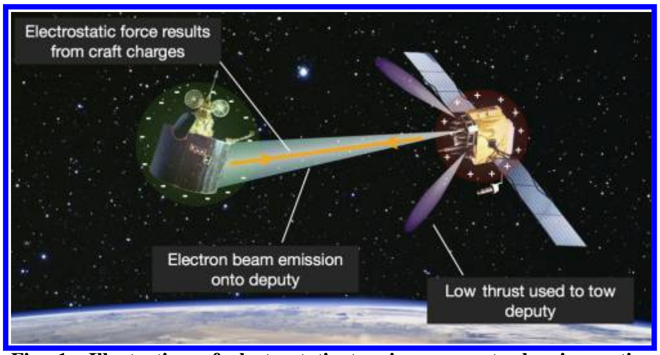

Fig. 1 Illustration of electrostatic tugging concept, showing active charge transfer with an electron beam.

charging capability. The second craft, denoted as the deputy, only possesses charging capabilities. The previous work with this electrostatic tugging concept considers only a nominal circular orbit, with the goal of increasing the semimajor axis of the deputy object. In the current paper, other orbit corrections are considered to reposition a passive space object in a more general way using an electrostatic tug. The first parameter considered is that of raising the radius of perigee with orbits that can have nonzero eccentricities. Although space debris mitigation is not the sole focus of this paper, this applies to a debris object that has been raised into a disposal orbit, but due to the addition of eccentricity has dropped back into the GEO belt. Other orbital elements under consideration, more applicable to a stationkeeping or general reorbiting maneuver, are eccentricity, inclination, and right ascension of the ascending node.

For this study, Gauss's variational equations are used [15]. Assuming the tug and deputy object positions are fixed relative to one another in the rotating Hill frame, the variational equations are integrated to obtain the average change in the orbital elements over one orbital period. The closed-loop control of the desired relative motion, a challenge which is studied in [13], is not considered in this study. Rather, of interest are the orbit element changing performance predictions and the associated voltage and vehicle size requirements. Candidate strategies for achieving the required tug direction are discussed because the tug direction changes during one orbit for some of the cases considered. The magnitude of the deputy acceleration is dependent on the debris mass and the voltage levels on both of the objects (tug and deputy).

II. Background

The electrostatic tug concept is illustrated in Fig. 1. A tug vehicle, equipped with inertial thrusters, approaches a deputy object. Once in place, both tug and deputy are charged to opposite polarity. If the deputy does not possess the capability of charge control, electron beam emission from the chief may be used for remote charging. This results in an attractive electrostatic force, which serves as a virtual tether connection between tug and deputy. The thrusters are then used to slowly tow the deputy object to perform orbital corrections. The magnitude of the electrostatic forces considered for the electrostatic tug concept are on the order of millinewtons, meaning that low-thrust engines are required to prevent the tug from breaking the electrostatic tether and pulling away from the deputy [5,13,16].

A. Electrostatic Force Model

The performance of the electrostatic tug is dependent on the electrostatic force in place between the tug and deputy. To allow for analytic modeling, the tug and deputy object are treated geometrically as spheres. The potential on the tug object is a result of its own charge and the potential due to the charged deputy object as [16]

$$V_t = k_c \frac{q_t}{r_t} + k_c \frac{q_d}{L} \tag{1}$$

where $k_c = 8.99 \times 10^9\ \mathrm{Nm^2/C^2}$ is the coulomb constant, L is the distance between tug and deputy, q_t is the charge on the tug, q_d is the charge on the deputy, and r_t is the radius of the tug craft. Unless otherwise noted, the tug radius is assumed to be 3 m throughout this paper. Similarly, the potential on the deputy object is computed as

$$V_d = k_c \frac{q_d}{r_d} + k_c \frac{q_t}{L} \tag{2}$$

where r_d is the radius of the deputy object.

If the potentials on the tug and deputy are controlled, then the preceding relationships may be rearranged to solve for charge [16]:

$$\begin{bmatrix} q_t \\ q_d \end{bmatrix} = \frac{L}{k_c(L^2 - r_t r_d)} \begin{bmatrix} r_t L & -r_t r_d \\ -r_t r_d & r_d L \end{bmatrix} \begin{bmatrix} V_t \\ V_d \end{bmatrix} \tag{3}$$

After computing the charges, the electrostatic force between tug and deputy is computed using

$$F_c = k_c \frac{q_t q_d}{L^2} \tag{4}$$

Note that this force may be either attractive or repulsive depending on the potentials of the tug and deputy. For the electrostatic tug application, the tug may be employed either in a pushing or pulling configuration. In the pushing configuration, a repulsive force is applied with the tug behind the deputy object. In the pulling configuration, an attractive force is used with the tug ahead of the deputy object. As detailed in [16], it is advantageous to use the pulling configuration in terms of electrostatic force magnitudes and stability of the tug–deputy alignment. In this study, only the pulling configuration will be considered, with tug and deputy charged to opposite polarity. Once the electrostatic force is computed, the deputy acceleration is simply

$$a_c = \frac{F_c}{m_d} \tag{5}$$

It is worth noting that the preceding electrostatic force model does not account for induced effects [17]. As two charged spheres are brought in close proximity, the charge distribution becomes nonuniform on the surfaces. In the case of opposite polarity, more charge will accumulate on the near sides of the spheres. When the spheres are the same polarity, the charges will accumulate more on the far sides of the spheres. This has the effect of increasing the electrostatic force for the attractive case and decreasing it in the case of repulsion. The induced charge effect, however, is most apparent at shorter separation distances of less than a few sphere radii. For some of the larger sizes of debris objects considered here, induced effects will contribute to an increase in the electrostatic force beyond what is predicted by the position-dependent capacitance model. Thus, the results for the larger debris objects considered in this study (>3500 kg) may be considered as a conservative lower bound on achievable reorbiting performance.

Because of the space weather environment, some shielding of this electrostatic force will occur. The distance over which this shielding is prevalent is described by the debye length of the local plasma [18]. The space weather conditions considered in this study yield debye lengths that are on the order of tens of meters. However, because of the high potential levels obtained by tug and deputy, the debye shielding effect will be several times smaller than predicted by the standard debye length calculation. As discussed in [19,20], objects charged to tens of kilovolts in the space environment experience effective debye lengths several times larger. Looking specifically at this phenomenon as it pertains to charging in quiet GEO space weather conditions, the effective debye lengths are predicted to be roughly five times larger than the classic debye shielding model predicts [20]. The shortest debye lengths considered here range from 15 to 35 m, leading to effective debye lengths over 75 m. This means that the space weather environment will not contribute significant shielding of the electrostatic force below distances of 75 m. Because the separation distances considered here are less than 20 m, the impacts of debye shielding are insignificant and will not be included in the force model.

For the electrostatic tugging concept to be feasible, both chief and deputy must possess the capability for charge control. If the deputy is not purpose designed for charge control, an extra requirement is placed on the tug. Without an inherent ability for self-charging, the deputy must be remotely charged by the chief [5]. This may be accomplished through the use of a charged-particle beam [14]. Consider, for example, an electron beam emitted by the tug. The outflow of negatively charged particles will result in a positive charge on the tug. Directing the beam onto the deputy object results in an influx of electrons that will charge the deputy to a negative polarity. Ultimately, an attractive force is achieved between the deputy and tug. In the current study, the mechanics of this charge transfer process are not considered. Rather, it is assumed that active charging of tug and deputy has been achieved.

The charge expressions in Eq. (3) require the radius of the deputy object. Considering that arbitrary deputy objects may be targeted for removal, a range of craft sizes must be considered to evaluate the performance of the electrostatic tug for general reorbiting maneuvers. In [16], publicly available data on geostationary satellites are used to obtain a relationship that relates mass m_d to an effective radius of the nearest spherical shape approximation. Because the objects considered are not truly spheres, the radii obtained are only approximations that allow for analytic charge predictions. The data considered result in the mean mass to radius relationship [16]

$$r_d(m_d) = \left(1.152\ \text{m} + 0.00066350\ \frac{\text{m}}{\text{kg}}\right) m_d \tag{6}$$

B. Variational Equations

To study the reorbiting capabilities of the electrostatic tug concept, Gauss's variational equations are used. In prior work, semimajor axis changes are considered for debris objects located at geosynchronous altitudes with the tug leading the deputy in the along-track direction [5,13,16]. Here, the electrostatic tugging research is extended in two ways: 1) by considering more general orbital element changes, as well as 2) considering the required relative tug/debris positions to achieve these maneuvers. The orbital position of the deputy object is assumed to be described by a set of osculating classical orbital elements: the semimajor axis a, eccentricity e, inclination i, right ascension of the ascending node Ω, argument of perigee ω, and true anomaly f [15].

The acceleration of the deputy due to the electrostatic force a_c is decomposed into components in the rotating Hill frame of the deputy, also referred to as the local-vertical local-horizontal frame: a_r, a_θ, and a_h. The a_r component is aligned with the orbit radius vector, the a_h component is aligned normal to the orbit plane, and the a_θ component acts orthogonal to a_r and a_h, in the along-track direction.

Gauss's variational equations provide the rates of change for the set of osculating orbit elements as [15]

$$\frac{\mathrm{d}a}{\mathrm{d}t} = \frac{2a^2}{h}\left(e \sin f a_r + \frac{p}{r} a_\theta\right) \tag{7a}$$

$$\frac{\mathrm{d}e}{\mathrm{d}t} = \frac{1}{h}(p \sin f a_r + ((p+r)\cos f + re)a_\theta) \tag{7b}$$

$$\frac{\mathrm{d}i}{\mathrm{d}t} = \frac{r\cos(\omega+f)}{h} a_h \tag{7c}$$

$$\frac{\mathrm{d}\Omega}{\mathrm{d}t} = \frac{r\sin(\omega+f)}{h\sin i} a_h \tag{7d}$$

$$\frac{\mathrm{d}\omega}{\mathrm{d}t} = \frac{1}{he}[-p\cos f a_r + (p+r)\sin f a_\theta] - \frac{r\sin(\omega+f)\cos i}{h\sin i} a_h \tag{7e}$$

$$\frac{\mathrm{d}f}{\mathrm{d}t} = \frac{h}{r^2} + \frac{1}{he}[p\cos f a_r - (p+r)\sin f a_\theta] \tag{7f}$$

where r is the orbit radius, $p = a(1-e^2)$ is the semilatus rectum, and $h = r^2\dot{f}$ is the orbit-specific angular momentum magnitude. Generally, these equations must be numerically integrated to determine how the osculating elements evolve with time. For the case of the electrostatic tug, however, a few assumptions are made that allow for analytic predictions of orbit element changes. First, the electrostatic force magnitudes are small (approximately millinewton or less) and do not create large changes in the orbital elements over one orbital period. Second, during the tugging maneuver, the relative position of the tug and deputy is held piecewise constant, meaning that the direction of a_c is also piecewise constant. Lastly, the assumption is made that the magnitude of the electrostatic force, and the corresponding acceleration, is constant throughout the maneuver.

With these assumptions, it is possible to predict how the orbital elements of the deputy object will evolve over one orbit without requiring numerical integration of the variational equations. By extending this prediction to multiple orbits, a reasonable approximation may be obtained for the performance of the electrostatic tug for general reorbiting maneuvers. To arrive at the analytic predictions, the procedure detailed in [21] is used. The independent variable in the variational equations is changed from time to eccentric anomaly, resulting in the modified rate equations [21]:

$$\frac{\mathrm{d}a}{\mathrm{d}E} = \frac{2a^{5/2}}{\mu\sqrt{p}}\left(ae\sqrt{(1-e^2)}\sin E a_r + p a_\theta\right) \tag{8a}$$

$$\frac{\mathrm{d}e}{\mathrm{d}E} = \frac{\sqrt{ap}}{\mu}\Big(a\sqrt{(1-e^2)}\sin E a_r + a(2\cos E - e - e\cos^2 E)a_\theta\Big) \tag{8b}$$

$$\frac{\mathrm{d}i}{\mathrm{d}E} = \frac{a^{5/2}}{\mu\sqrt{p}}\left(\cos\omega(\cos E - e) - \sqrt{1-e^2}\sin\omega\sin E\right)(1 - e\cos E)a_h \tag{8c}$$

$$\frac{\mathrm{d}\Omega}{\mathrm{d}E} = \frac{a^{5/2}}{\mu\sqrt{p}}\left(\sin\omega(\cos E - e) + \sqrt{1-e^2}\cos\omega\sin E\right)(1 - e\cos E)a_h \tag{8d}$$

Note that the argument of perigee and true anomaly equations have been omitted because they will not be used here.

Using the assumptions outlined previously, the only term in Eq. (8) that changes significantly over one orbital period is the eccentric anomaly E. An analytic expression for the orbit element changes over one orbital period is obtained by integrating Eq. (8) on the interval $E = [0, 2\pi]$. In this study, four different scenarios are considered. The first is a change in radius of perigee, with a focus on debris reorbiting applications. International guidelines call for debris in the GEO belt to be raised to a higher disposal orbit [22,23]. Over time, solar radiation pressure will introduce eccentricity into the disposal orbit of a debris object. If this eccentricity is large enough, the radius of perigee of the orbit may dip back into the GEO belt. Here, we consider how much effort is required to raise the radius of perigee back to a safe altitude. Beyond the radius of perigee corrections, changes in eccentricity, inclination, and right ascension of the ascending node are considered. Such orbital element corrections are more suitable for a nondebris-related scenario where a change in the deputy orbit is called for.

III. Orbit Modification Predictions

In this section, analytic predictions are made for the various orbit modifications considered in this study. The electrostatic force expression in Eq. (4) is computed for a range of vehicle sizes and potential levels. Different separation distances are also considered. Sweeping these parameters allows for the computation of performance predictions for a wide range of cases. For each of the orbit element corrections, maneuvers are designed such that changes occur only to the orbital parameter considered out of the four (r_p, e, i, Ω). For example, when considering inclination changes, the tug craft is placed such that only inclination is changed over one orbit. Designing the maneuvers in this way requires a repositioning of the tug craft during the orbit in certain cases. This issue will be discussed shortly.

A. Radius of Perigee Corrections

Here, the work is motivated by a debris mitigation scenario in the GEO regime. As discussed earlier, a situation is conceivable in which a once-circular disposal orbit has dipped back into the GEO belt due to an injection of eccentricity. Rather than recircularizing and increasing the orbit radius, a simpler solution would be to increase the radius of perigee. This would only raise the lowest debris orbit point to be outside the GEO zone, without wasting fuel raising the already acceptable apogee location. The radius of perigee is defined as

$$r_p = a(1 - e) \tag{9}$$

Taking the derivative of this expression with respect to the eccentric anomaly yields

$$\frac{\mathrm{d}r_p}{\mathrm{d}E} = \frac{\mathrm{d}a}{\mathrm{d}E}(1 - e) - a\frac{\mathrm{d}e}{\mathrm{d}E} \tag{10}$$

Using the relationships in Eq. (8), the rate of change of the radius of perigee with respect to the eccentric anomaly is found to be

$$\frac{\mathrm{d}r_p}{\mathrm{d}E} = \frac{2a^3}{\mu}\left(-(e-1)^2\cos\left(\frac{E}{2}\right)\sin\left(\frac{E}{2}\right)a_r + \sqrt{1-e^2}(2 - e - e\cos E)\sin^2\left(\frac{E}{2}\right)a_\theta\right) \tag{11}$$

To assess performance of the electrostatic tug for raising the radius of perigee, Eq. (11) is integrated from $E = [0, 2\pi]$ to determine the change in r_p over one orbit. The result of this integration is

$$\Delta r_p = \frac{\pi a^3}{\mu}(4 - e)\sqrt{1 - e^2}a_\theta \tag{12}$$

This equation illustrates that higher eccentricity values will hinder the performance of the radius-of-perigee-raising maneuver. If the tug is held at a constant position throughout an orbit, as is assumed here, only the electrostatic force component in the along-track direction will affect the radius of perigee. To maximize the force in this direction, the best configuration is one where the tug is ahead of the debris object in the along-track direction (the leader–follower alignment). If this configuration is adopted, then $a_\theta = a_c$.

Performance of the radius-of-perigee-raising maneuver is considered for two separation distances: $L = 10$ and 15 m. For each separation distance, deputy masses ranging from 300 to 5000 kg are included. The voltage on the tug and debris is assumed to be of equal magnitude, but opposite polarity. The debris object is assumed to have been initially reorbited to a disposal orbit 300 km above GEO, but due to the injection of eccentricity had dropped its radius of

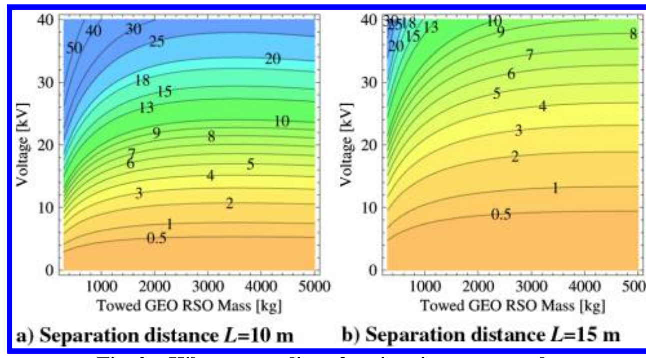

Fig. 2 Kilometer radius of perigee increase per day.

perigee back into the GEO belt. This results in an eccentricity of 0.00359 and a semimajor axis of 42,391 km for the debris orbit. The amount of increase in the radius of perigee per orbit for these various conditions is shown in Fig. 2. Here, the nomenclature of resident space object (RSO) is used, where RSO may refer to a towed debris or cooperative deputy object.

In general, closer separation distances and higher voltage levels lead to larger increases in r_p over one orbital period. These trends are due to the increased magnitude of electrostatic forces that result from higher potentials and smaller L values. Furthermore, note that the contour lines do not continuously increase as the RSO mass grows larger. This is indicative of the higher capacitance available on larger objects, which have higher surface areas. This increased capacitance results in larger charge magnitudes for the same potential, in turn increasing the magnitude of the electrostatic force between tug and debris. The results here indicate that, if separation distances on the order of 10–15 m are maintained, along with potential levels between 20 and 30 kV, the radius of perigee of the debris object may be increased by 300 km over a period of a few months.

B. Eccentricity Corrections

Let us now turn our attention to eccentricity changes, which may be part of general orbit corrections for a deputy object. Here, a modification of eccentricity is desired where the other orbit elements remain unchanged after one orbital period. This can be accomplished by switching the sign of a_θ, which is assumed to equal a_c, when $E = \pm\pi/2$ [21]. This corresponds to moving the tug from ahead to behind the deputy object and back during each orbit. During this repositioning time, it is assumed that the tug will discharge, meaning no electrostatic force is present. If the tug can be repositioned quickly enough, the impact on the overall eccentricity change will be minimal. If this procedure is carried out, assuming minimal effects due to the repositioning maneuver, the eccentricity change over one orbital period is approximately [21]

$$\Delta e = \frac{8a^2}{\mu}\sqrt{1 - e^2}a_c \tag{13}$$

Again, a debris object at GEO altitudes with a slight eccentricity is considered. Here, the semimajor axis of the debris orbit is assumed to be 42,391 km with an eccentricity of 0.00359. Performance for various separation distances, RSO masses, and potential levels are considered, again using the mass to radius ratio in Eq. (6). The results are shown in Fig. 3. Similar trends as before are noted, where performance is improved by closer separation distances and higher potential levels. Considering the predictions shown here, the orbit of the modeled deputy object could be recircularized over a period of one to three months, depending on the separation distance, potential, and mass. Note that this corresponds to a change in position of a few hundred kilometers, which is a similar performance result as the radius of perigee corrections over a similar time frame.

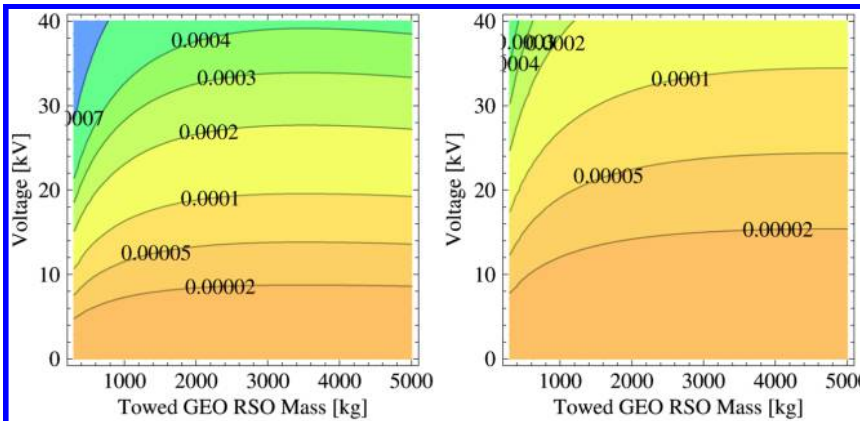

a) Separation distance L=10 m b) Separation distance L=15 m

Fig. 3 Eccentricity change per day.

C. Inclination Corrections

For the inclination corrections, a maneuver is sought in which only the inclination is changed after one orbital period. This may be accomplished by repositioning the tug during the orbit at $\omega + f = \pm\pi/2$ [21]. For pure inclination changes, the tug needs to be moved from above to below (or vice versa) the deputy orbital plane at these locations in the orbit. Again, it is assumed that this repositioning will occur quickly enough that minimal impact occurs on the inclination change performance, so that an instantaneous repositioning is a valid assumption. Maintaining the tradition of assuming small deputy object eccentricity, the approximate change over one orbital period using this repositioning maneuver is [21]

$$\Delta i = \frac{4a^2}{\mu} a_c \tag{14}$$

Eccentricity does not appear in this expression because of the near-circular orbit assumption.

To assess performance of tug for inclination changes, two separation distances are considered: $L = 10$ and 15 m. The same ranges of voltages and masses are considered as before, and the deputy is assumed to be in an orbit with a semimajor axis of 42,241 km. The results are shown in Fig. 4. In general, modifications to the inclination of no more than a few thousandths of a degree are possible over one orbit. Even over a time period of a few months, it is not possible to achieve inclination changes of 1 deg. The low performance of the electrostatic tug for inclination changes can be attributed to the large ΔV typically required to perform such corrections. The electrostatic forces acting on the deputy are very small (on the order of millinewtons) and are not available at a magnitude significant enough to greatly affect the inclination.

D. Right Ascension of the Ascending Node Corrections

For modifications to the right ascension of the ascending node (RAAN), a maneuver is considered that results in only RAAN changes after one orbit. This may be accomplished by reversing the direction of the electrostatic force at each equatorial crossing ($\omega + f = 0$) [21]. Again, this requires a repositioning of the tug twice per orbit. It is assumed that this repositioning occurs quickly enough so that it will have negligible impact on the amount of RAAN change. Integrating the rate of change of RAAN in Eq. (8) across one orbit, assuming both a small eccentricity and the aforementioned changes in electrostatic force direction, yields a change per orbit of [21]

$$\Delta\Omega = \frac{4a^2}{\mu \sin i} a_c \tag{15}$$

Here, the inclination of the deputy orbit has a direct impact on the performance of the tug. Smaller inclinations will result in larger changes in Ω for the same a_c.

The performance of the tug for RAAN changes is computed assuming an inclination of 5 deg. Two separation distances are considered, $L = 10$ and 15 m, and the semimajor axis of the orbit is assumed to be $a = 42,241$ km. The changes in RAAN for a range of RSO masses and craft voltages are shown in Fig. 5. The potential RAAN changes over a period of a few months are on the order of several degrees for the cases considered here. This is much more significant than the possible inclination changes. However, the deputy object inclination is assumed to be relatively small here. Larger inclinations would significantly hinder the potential of the electrostatic tug to perform RAAN corrections.

E. Tug Repositioning Considerations

In the evaluation of orbit element modification performance, tug repositioning maneuvers are assumed for changes in e, i, and Ω. During the repositioning phase of the orbit, the tug is discharged so that no electrostatic force is in place between tug and deputy object. The primary reason for doing this is to prevent accelerations from acting on the deputy object in unwanted directions as the tug

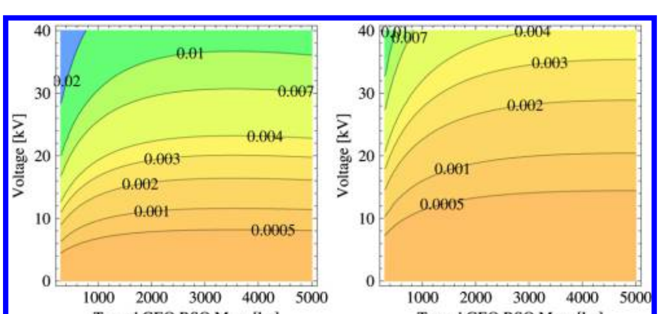

a) Separation distance L=10 m b) Separation distance L=15 m

Fig. 4 Inclination change per day (in degrees).

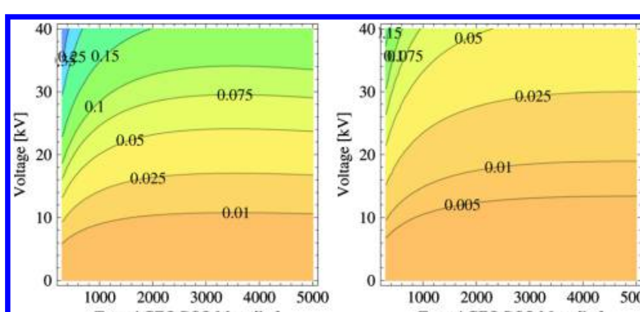

a) Separation distance L=10 m, $i = 5°$ b) Separation distance L=15 m, $i = 5°$

Fig. 5 RAAN change per day (in degrees).

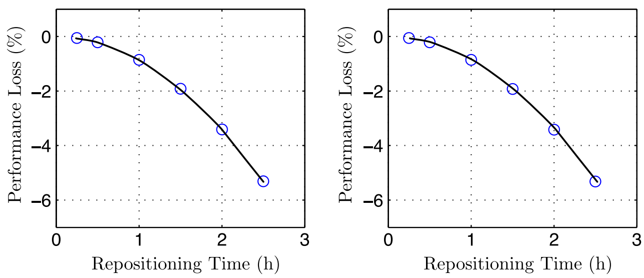

a) Eccentricity **b) Raan**

Fig. 6 Percent loss in performance over one orbital period for various repositioning times.

maneuvers around it. These unintended accelerations would lead to changes in orbital elements that are not desired.

F. Performance Losses

In the following analysis, a deputy object with a semimajor axis of 42,241 km and an eccentricity of 0.001 is considered. The inclination is set at 5 deg, the right ascension of the ascending node at 20 deg, and the argument of perigee at 90 deg. For these conditions, the orbital period will be approximately 24 h. The deputy object is assumed to have a mass of 2000 kg and a potential of -25 kV. The tug is assumed to be at a potential of 25 kV with a radius of 3 m. The nominal separation distance is set at 15 m. To determine the impact of tug repositioning on performance, numerical simulation of the inertial equations of motion is used. Here, only the motion of the deputy is propagated with

$$\ddot{\boldsymbol{r}}_d = -\frac{\mu}{r_d^3}\boldsymbol{r} + \boldsymbol{a}_c \tag{16}$$

where $\boldsymbol{a}_c$ is computed using Eq. (5). The direction of $\boldsymbol{a}_c$ is set depending on which orbital element is being corrected. To simulate the tug repositioning, $\boldsymbol{a}_c$ is set to zero for various time spans during an orbit where the repositioning occurs. The tug reorientation is divided equally on either side of the switching condition. For example, if an eccentricity change maneuver is considered, then half of the tug repositioning occurs on one side of $E = \pi/2$ and the remainder on the other side. Effectively, the switching condition is encountered when the tug is halfway through repositioning.

The finite-time tug realignment maneuvers are compared with an instant realignment, as assumed in the performance predictions in the preceding section. The percent loss in performance for various repositioning times is computed for eccentricity and RAAN corrections. The results are shown in Fig. 6. Note that the repositioning times shown here are for a single repositioning maneuver, which occurs twice per orbit. So, for a 2.5 h maneuver time, there are a total of 5 h during the orbit during which no electrostatic force acts on the deputy. This is slightly more than 20% of the orbit. Even for such a large fraction of the orbital period, the performance losses are relatively minimal at slightly more than 5%. The reason for this is that the switching conditions occur at times in the orbit when the rates of change for their respective orbital elements are nearly zero. The penalty for removing the electrostatic force at these locations is minimal because there is already little change of the orbital element. As the repositioning time is increased, however, the penalties increase because regions of the orbit with higher rates of orbital element changes are encountered. The results of this analysis indicate that, practically, the repositioning will have minimal impact on the overall performance of the electrostatic tug.

IV. Conclusions

This paper assesses the capabilities of the electrostatic tug concept for performing various orbital corrections on a deputy object. Variational equations are used to analytically predict the amount of orbital element changes possible for various masses, charge levels, and separation distances. The time required to perform a slot change in a GEO orbit is also computed. The orbits considered for the deputy object are all of low eccentricity (~0.001 or less). The spacecraft are treated as idealized conducting spheres, and it is assumed that they possess the capability for charge control to the levels considered. Large-scale corrections are not possible in a short time span due to the small magnitudes of the electrostatic forces considered. Still, radius of perigee changes of several hundred kilometers are possible over several months, and low eccentricity orbits may be recircularized in similar timeframes. The worst performance is observed for inclination changes, owing to the large ΔV required to perform such corrections. The force magnitudes considered here are not sufficient enough to increase or decrease inclination by even 1 deg in a few months' time. For several of the orbit element corrections, maneuvers are considered where tug repositioning is required during each orbit. Numerical simulation is used to determine the effects of repositioning on performance. For repositioning times of up to 2.5 h, no more than 5.5% of performance loss occurs.

Acknowledgment

The authors would like to thank Bo Naasz for insightful conversations on the subject of the electrostatic tug concept and potential applications.

References

[1] King, L. B., Parker, G. G., Deshmukh, S., and Chong, J.-H., "Spacecraft Formation-Flying Using Inter-Vehicle Coulomb Forces," NASA Inst. for Advanced Concepts, Jan. 2002.

[2] King, L. B., Parker, G. G., Deshmukh, S., and Chong, J.-H., "Study of Interspacecraft Coulomb Forces and Implications for Formation Flying," *Journal of Propulsion and Power*, Vol. 19, No. 3, 2003, pp. 497–505.
doi:10.2514/2.6133

[3] Hussein, I. I., and Schaub, H., "Invariant Shape Solutions of the Spinning Three Craft Coulomb Tether Problem," *Journal of Celestial Mechanics and Dynamical Astronomy*, Vol. 96, No. 2, 2006, pp. 137–157.
doi:10.1007/s10569-006-9043-8

[4] Seubert, C. R., and Schaub, H., "Tethered Coulomb Structures: Prospects and Challenges," *Journal of Astronautical Sciences*, Vol. 57, Nos. 1–2, Jan.–June 2009, pp. 347–368.
doi:10.1007/BF03321508

[5] Schaub, H., and Moorer, D. F., "Geosynchronous Large Debris Reorbiter: Challenges and Prospects," *AAS/AIAA Kyle T. Alfriend Astrodynamics Symposium*, American Astronautical Soc. Paper 2010-311, May 2010.

[6] Cover, J. H., Knauer, W., and Maurer, H. A., "Lightweight Reflecting Structures Utilizing Electrostatic Inflation," U.S. Patent 3,546,706, Oct. 1966.

[7] Pettazzi, L., Izzo, D., and Theil, S., "Swarm Navigation and Reconfiguration Using Electrostatic Forces," *Seventh International Conference on Dynamics and Control of Systems and Structures in Space*, Greenwich, England, U.K., July 2006, pp. 257–267.

[8] Natarajan, A., and Schaub, H., "Orbit-Nadir Aligned Coulomb Tether Reconfiguration Analysis," *Journal of Astronautical Sciences*, Vol. 56, No. 4, Oct.–Dec. 2008, pp. 573–592.
doi:10.1007/BF03256566

[9] Wang, S., and Schaub, H., "Nonlinear Charge Control for a Collinear Fixed Shape Three-Craft Equilibrium," *Journal of Guidance, Control, and Dynamics*, Vol. 34, No. 2, March–April 2011, pp. 359–366.
doi:10.2514/1.52117

[10] Schaub, H., Parker, G. G., and King, L. B., "Challenges and Prospects of Coulomb Spacecraft Formation Control," *Journal of Astronautical Sciences*, Vol. 52, Nos. 1–2, 2004, pp. 169–193.

[11] Lai, S. T., "Overview of Electron and Ion Beam Effects in Charging and Discharging of Spacecraft," *IEEE Transactions on Nuclear Science*, Vol. 36, No. 6, 1989, pp. 2027–2032.
doi:10.1109/23.45401

[12] Mullen, E. G., Gussenhoven, M. S., and Hardy, D. A., "SCATHA Survey of High-Voltage Spacecraft Charging in Sunlight," *Journal of Geophysical Research: Space Physics*, Vol. 91, No. A2, 1986, pp. 1074–1090.

[13] Hogan, E., and Schaub, H., "Relative Motion Control for Two-Spacecraft Electrostatic Orbit Corrections," *Journal of Guidance, Control, and Dynamics*, Vol. 36, No. 1, Jan.–Feb. 2013, pp. 240–249.
doi:10.2514/1.56118

[14] Schaub, H., and Sternovský, Z., "Active Space Debris Charging for Contactless Electrostatic Disposal Maneuvers," *Sixth European Conference on Space Debris*, European Space Agency Paper 6b.O-5, April 2013.

[15] Schaub, H., and Junkins, J. L., *Analytical Mechanics of Space Systems*, AIAA Education Series, 2nd ed., AIAA, Reston, VA, Oct. 2009, pp. 591–596.

[16] Schaub, H., and Jasper, L. E. Z., "Orbit Boosting Maneuvers for Two-Craft Coulomb Formations," *Journal of Guidance, Control, and Dynamics*, Vol. 36, No. 1, Jan.–Feb. 2013, pp. 74–82. doi:10.2514/1.57479

[17] Soules, J. A., "Precise Calculation of the Electrostatic Force Between Charged Spheres Including Induction Effects," *American Journal of Physics*, Vol. 58, No. 12, 1990, p. 1195. doi:10.1119/1.16251

[18] Bittencourt, J., *Fundamentals of Plasma Physics*, Springer–Verlag, New York, 2004, pp. 7–9.

[19] Murdoch, N., Izzo, D., Bombardelli, C., Carnelli, I., Hilgers, A., and Rodgers, D., "Electrostatic Tractor for Near Earth Object Deflection," *59th International Astronautical Congress*, Vol. 29, International Astronautical Federation IAC-08-A3.I.5, Paris, 2008.

[20] Stiles, L. A., Seubert, C. R., and Schaub, H., "Effective Coulomb Force Modeling in a Space Environment," *AAS Spaceflight Mechanics Meeting*, American Astronautical Soc. Paper 12-105, Jan.–Feb. 2012.

[21] Burt, E., "On Space Manoeuvres with Continuous Thrust," *Planetary and Space Science*, Vol. 15, No. 1, Jan. 1967, pp. 103–122. doi:10.1016/0032-0633(67)90070-0

[22] "IADC Space Debris Mitigation Guidelines," Interagency Space Debris Coordination Com. TR-IADC-02-01, 2007.

[23] "NASA Safety Standard: Guidelines and Assessment Procedures for Limiting Orbital Debris," NASA TR-NSS-1740.14, 1995.